CrossMark

Effects of Particle Size Non-Uniformity on Transport and Retention in Saturated Porous Media

**Ahmed Hammadi[1] · Nasre-Dine Ahfir[1] ·
Abdellah Alem[1] · HuaQing Wang[1]**

Abstract Short-pulse injection experiments are investigated to study the effects of particle size non-uniformity on the transport and retention in saturated porous media. Monodisperse particles (3, 10, and 16 μm latex microspheres) and polydisperse particles (containing 3, 10, and 16 latex microspheres) were explored. The obtained results suggest considering not only the particle sizes but also their polydispersivity (particle size non-uniformity) in transport and retention. Although, the density of the suspended particles is close to that of water, results reveal a slow transport of particles compared to the dissolved tracer whatever their size and flow velocity. The recovered particles in the mixture experiments show that the retention of large particles (10 and 16 μm) enhances the retention of small ones (3 μm). However, the straining of 10 and 16 μm particles in "mixture experiments" is smaller than their straining in "monodisperse experiments". A linear relationship summarizing the simultaneous effect of particle sizes and flow velocity on deposition kinetics coefficient is proposed.

1 Introduction

Solid particles transport and deposition are frequently encountered phenomena in a wide range of industrial and natural processes. In groundwater, solid particles might be intrinsic pollutants or can facilitate the contaminants mobility by carrying them much faster and further than predicted with a traditional solute transport. Otherwise, these particles can remain a barrier or retard the migration of pollutants if their presence clogs the porous medium

✉ Nasre-Dine Ahfir
ahfirn@univ-lehavre.fr

[1] UMR 6294 CNRS, LOMC, Normandie Univ, UNIHAVRE, 76600 Le Havre, France

(Kretzschmar et al. 1999; Sen et al. 2002; McCarthy and McKay 2004; Sen and Khilar 2006; Walshe et al. 2010; Syngouna and Chrysikopoulos 2013). In water and wastewater treatment, the filtration through granular media is largely used to remove micron-sized particles from liquid input streams (Aim et al. 1997; Sadiq et al. 2003). In petroleum engineering, the water injected through the reservoir contains suspended particles which can deposit in the well and cause a decrease in productivity (Moghadasi et al. 2004). In civil engineering, the release of soil particles can lead to internal erosion of the hydraulic structures and cause their breakdown (Bonelli et al. 2006; Clark and Wynn 2007; Sjödahl et al. 2008).

Solid particles in the subsurface environment may be of several types: inorganic, organic, and microbiological particles. The transport of colloidal particles ($d_p \leq 1 \ \mu m$) in porous media has been widely studied because of their abundance in groundwater and their physical properties (McCarthy and McKay 2004; McDowell-Boyer et al. 1986). Recent studies have investigated the transport and deposition of suspended particles ($d_p > 1 \ \mu m$) in saturated porous media (Masséi et al. 2002; Benamar et al. 2005; Ahfir et al. 2009; Bennacer et al. 2013; Chen and Bai 2015).

Several transport, deposition, and remobilization mechanisms control particle transport in porous media, such as physicochemical conditions (Chen et al. 2011; Ryan and Elimelech 1996; Mesticou et al. 2016), particle size (Herzig et al. 1970; Bradford et al. 2003; Bennacer et al. 2013), concentration of injected particles (Lee and Koplik 2001; Alem et al. 2013), porous media grain size (Porubcan and Xu 2011; Ahfir et al. 2016), and the grain surface (Torkzaban et al. 2010; Sefrioui et al. 2013). Various restrictions on the movement of solid particles such as straining and filtration have been studied (Bradford et al. 2003; Xu and Saiers 2009; Porubcan and Xu 2011; Alem et al. 2013). The straining depends essentially on the ratio between particle diameter (d_p) and grain diameter (d_g). In the literature, different critical values of d_p/d_g, beyond which the straining become the dominant capture mechanism, are suggested. Bradford et al. (2002) and Xu et al. (2006) proposed a critical value of d_p/d_g equal 0.002 and 0.008, respectively. More recent work (Tosco and Sethi 2010; Raychoudhury et al. 2014) observed that the straining can play a prominent role in particles retention even for much lower values of d_p/d_g (about 0.0002). Those authors explained this behaviour by the formation of aggregates that enhance the straining. Bradford et al. (2007) observed that the straining increases when the ionic strength increases and that it decreases when the flow velocity increases. However, the magnitude of the effect of flow velocity is expected to be highly dependent on the solution chemistry and the size of the colloid and porous medium grain. Several studies showed that the straining of solid particles is more significant at the entrance of the porous media (Johnson et al. 2007; Bradford et al. 2003, 2007; Alem et al. 2013).

Most previous studies on solid particles transport and deposition were conducted using monodisperse particles (Bradford et al. 2003; Xu et al. 2008; Porubcan and Xu 2011; Tong and Johnson 2006). However, the particles in natural soils have very heterogeneous size. Thus, describing and predicting polydispersive particle size behaviour in porous media are essential to a better understanding of their transport and deposition. Among the earlier studies focused on the polydispersive particles transport in fractured media the research of James et al. (2005) and James and Chrysikopoulos (2003, 2011). Brow et al. (2005) and Xu and Saiers (2009) studied the transport and deposition of bidisperse particles in saturated porous media.

This paper aimed to highlight the effect of particle size non-uniformity on the transport and retention of the suspended particles in porous media under different flow velocities. Three monodisperse particles were used, and a forth one (polydisperse suspension) was obtained from mixing the first three monodisperse particles with the same volume ratio. Laboratory pulse injection experiments were carried out in a column. The porous medium performance on the suspended particles removal was analysed with the aid of suspended

particles breakthrough curves (BTCs), hydrodispersive parameters of the porous medium, and the particle size distribution in the effluent.

2 Materials and Methods

2.1 Column Transport Experiments

The experimental system used in this study was similar to that presented in Bennacer et al. (2013). A plexiglass column with an inner diameter of 4.4 cm and a length of 32 cm was used. The column is fed by a reservoir containing pure water (pH of 6.7 ± 0.2) with 1 mM NaCl. A peristaltic pump (Cole-Parmer Masterflex) was placed at the entrance of the column to ensure a constant flow rate. The column was equipped with four pressure sensors (Measurement Specialities (France)) for measuring the pressure variation along the column. The detection system consists of a spectrometer (AstraSagitta UV/VIS) placed at the immediate outlet of the porous medium. The suspended particle (SP) and the dissolved tracer (DT) concentrations in the effluent were determined with the help of calibration curves establishing the relationship between measured SP/DT concentrations in the water and values in absorbance given by the spectrometer (wavelength absorbance for both SP and DT equals 490 nm).

Carboxylate-modified polystyrene latex microspheres (Invitrogen Thermo Fisher Scientific) with negative surface charge were used as SP. The size of these particles is provided by the manufacturer. The particle density is very close to that of water (1.05 g/cm^3), which enables to neglect the gravity effect. Three monodisperse populations of latex were used 3, 10, and 16 µm. For each experiment, the influent concentration was 6 g/L. The corresponding particle numbers were 4.04×10^8, 1.09×10^7, and 2.66×10^6 particles/mL for the population 3, 10, and 16 µm, respectively. To study the effect of polydispersivity of the injected particles, a fourth population (noted Mixture) is prepared by mixing the populations 3, 10, and 16 µm in equal volume proportion. Notice that the numbers of the particles of 3 µm in the Mixture population are 37 and 150 times more numerous than those of the population 10 and 16 µm, respectively. The zeta potential of these particles was measured by using a zetameter (ZetaCompact—CAD instrument). The average value of zeta potential was $-55.0 (\pm 5.6)$ mV.

Fluorescein was used as a DT in order to compare solute transport behaviour with that of the SP. A 5-mL syringe was filled of the tracer solution and placed in the immediate inlet of the column used to perform pulse injections. The injected pulse is very small (1 mL) with respect to pore volume (<0.6% pore volumes) in order not to disturb the water flow in the porous medium.

Quartz sand was used as the porous medium in-filling the column in the experiments. The grain size distribution of the sand is ranged between 630 and 800 µm and the median grain diameter $d_g = 715$ µm. Its bulk density, uniformity coefficient C_u, and average porosity were 1.58 g/cm^3, 1.37, and 0.393 (± 0.005), respectively. The sand was cleaned to remove all organic matter and fine particles attached to the grains. After repeated washing with pure water, the sand was soaked within nitric acid at a concentration of 0.01 M for 24 h, followed by rinsing with pure water. After that, it was soaked in NaOH (concentration of 0.1 M) for 6 h. Finally, the sand was washed with pure water until the electrical conductivity of the rinse water was less than 1 µS/cm. The sand is then dried for 24 h in an oven at 105 °C. The zeta potential of the porous medium used in this investigation was measured by using a zetameter (ZetaCAD-CAD Instruments), and its value was -25.3 mV (± 2.6). To simulate water flowing in groundwater, the column was installed in horizontal position. The average

hydraulic conductivity value of the porous media was 3.06×10^{-3} m/s ($\pm 3.410^{-4}$). Prior to each experiment, the porous media was flushed with 3 V_p of water.

Six flow velocities (0.035, 0.074, 0.100, 0.132, 0.160, and 0.200 cm/s) were tested for each SP/DT tracer. All the experiments were carried out in triplicate in order to improve the reproducibility of obtained results.

As discussed above, the recovery rates of the SP at the outlet of porous medium were determined using a previously calibrated spectrometer to SP concentration. A second method was used to evaluate the recovery rate of the SP by using a Coulter Multisizer counter. The method consists to measure the number of particles entirely transported to the outlet the porous medium. The ratio between the number of the recovered particles and the number of particles initially injected allows the determination of the recovery rate. This recovery rate is compared to that obtained by spectrometer, and an error less than 5% was measured.

As mentioned above, to evaluate the influence of particle polydispersivity on the retention, the Mixture population was injected in the same conditions than that performed with monodisperse particles (3, 10, and 16 µm). A comparison of the recovery rates of monodisperse particles in "monodisperse experiments" with that of particles constituting the Mixture population in "mixture experiments" was realized. A total of 72 experiments were performed. To assess the recovery rates of each SP population injected in the porous medium (monodisperse experiments and mixture experiments), particles numbers were counted using the Coulter Multisizer.

2.2 Electrostatic Interaction Energy Calculation and Forces Evaluation

In our experimental conditions, the deposition of particles through the porous media is governed by straining. To support this assumption, we calculated the interaction energy profiles, made by summation of equations for electrical double-layer (Φ_{EDL}), van der Waals interaction (Φ_{VDW}), and Born repulsion (Derjaguin and Landau 1941; Verwey and Overbeek 1948; Elimelech et al. 1995). The interaction energy profiles, the detailed equations for the interaction energy and forces, and the equation of the hydrodynamic force are given in Supporting Information.

Table S1 in Supporting Information provides calculated values of the repulsive energy barrier height (Φ_{max}), the depth of the primary energy minimum (Φ_{1min}), and the depth of the second energy minimum (Φ_{2min}) for all tested populations. The results show that the greater particle size, the more important the depth of the primary minimum and the second minimum. Also, the height of the energy barrier (Φ_{max}) decreases with decreasing the particle size. Table S1 also provides the ratios of the various interaction forces (adhesive forces F_{A1}, F_{A2}, and repulsive force F_B) to the hydrodynamic force (F_H) for two flow velocities (the lowest and highest velocity) for all tested SP populations (cf. Supporting Information). The values show that the adhesion forces calculated in the second minimum (F_{A2}) are negligible compared to hydrodynamic forces F_H ($F_{A2} \leq 0.003 F_H$). The repulsive force (F_B) and the adhesion force (F_{A1}) exceed the hydrodynamic forces (F_B varies between 7 and 146 times F_H). These results indicate that whatever the size and the flow velocities explored in this study, the hydrodynamic forces (F_H) are insufficient to overcome the energy barrier to fix the particle at the primary minimum. Thus, the physicochemical deposition plays a negligible role in this study.

3 Results and Discussion

The interpretation of the experimental data was realized with the help of the convection–dispersion equation with a first-order deposition kinetics (Kretzschmar et al. 1997; Grolimund

et al. 1998; Wang et al. 2000). Considering the experimental conditions used in this study: short-pulse injection technique with sufficiently low particle injected and constant flow rate; the particles release is neglected. Thus, the analytical solution of the convection–dispersion equation is given as follows (Wang et al. 2000):

$$C(t, x) = \frac{mx}{Q\sqrt{4\pi D_L t^3}} \exp(-K_{\text{dep}} t) \exp\left(-\frac{(x - ut)^2}{4D_L t}\right) \tag{1}$$

where C is the particle concentration in solution $[ML^{-3}]$, D_L is the hydrodynamic longitudinal dispersion coefficient $[L^2 T^{-1}]$, u is the average pore water velocity $[LT^{-1}]$, K_{dep} is the deposition kinetics coefficient $[T^{-1}]$, x is the distance $[L^{-1}]$, t is the time $[T]$, m is the mass of the particles initially injected $[M]$, and Q is the flow rate $[L^3 T^{-1}]$.

Based on the analytical solution (Eq. 1), the regression parabolic method (Bennacer et al. 2013) is used to interpret the breakthrough data. This method allows immediate determination of the dispersion coefficient, the convection time, and the deposition kinetics coefficient.

3.1 Transport Behaviour

Figure 1 presents experimental and fitted BTCs of both SP and DT for two flow velocities. The BTCs are represented by the relative concentration C_R versus the number of pore volumes NV_p:

$$C_R = \frac{NV_p.C}{V_{\text{inj}}.C_0} = \frac{\int_0^\infty Q.C.\mathrm{d}t}{V_{\text{inj}}.C_0} \tag{2}$$

$$NV_p = \frac{Q.t}{V_p} \tag{3}$$

where V_{inj} is the solute injected volume $[L^3]$, V_p is the pore volume of the porous medium $[L^3]$, and C_0 is the initial concentration $[ML^{-3}]$.

The experimental BTCs are fitted according to the analytical solution (Eq. 1). We observe that the BTCs are well represented by the model.

The BTCs show a clear asymmetry with a tail at the end of the breakthrough for all populations, regardless the flow velocity. For all velocities, the first SP arrives at the outlet of the porous medium after 0.9 V_p injected. The concentration reaches the peak after 1.3 V_p injected. The peak of the SP BTCs increases with decreasing particle size. The time to return to $C_R = 0$ (descending part of the BTCs) is faster for larger particles, and this time is around 4.3, 3.6, and 3.1 V_p for the population 3, 10, and 16 μm, respectively. BTCs tail can be explained by the collisions of a fraction of the transported particles with the grains of the porous medium without attachment owing to the unfavourable physicochemical conditions. As a result of repeated collisions, particles deviate and change trajectories (Fig. 2). SP transfer paths become, as a consequence, more complex and tortuous leading to a significant delay in their transport.

A shift between DT BTCs and those of SP is also shown in Fig. 1. The DT arrives at the porous medium outlet after 0.8 V_p injected and to the peak after 1 V_p injected (Cf. Fig. 1); then, the BTCs return to $C_R = 0$ after 1.4 V_p. A retardation factor t_r is defined as the ratio between the DT residence time (t_{DT}) and the SP residence time (t_{SP}). Figure 3 displays the variation in the retardation factor t_r as a function of the flow velocity U for all tested SP populations. Whatever the flow velocity and the population tested, t_r is always larger than 1, it varies between 1.5 and 2.0. As discussed above (Cf. Fig. 2), this behaviour can be explained
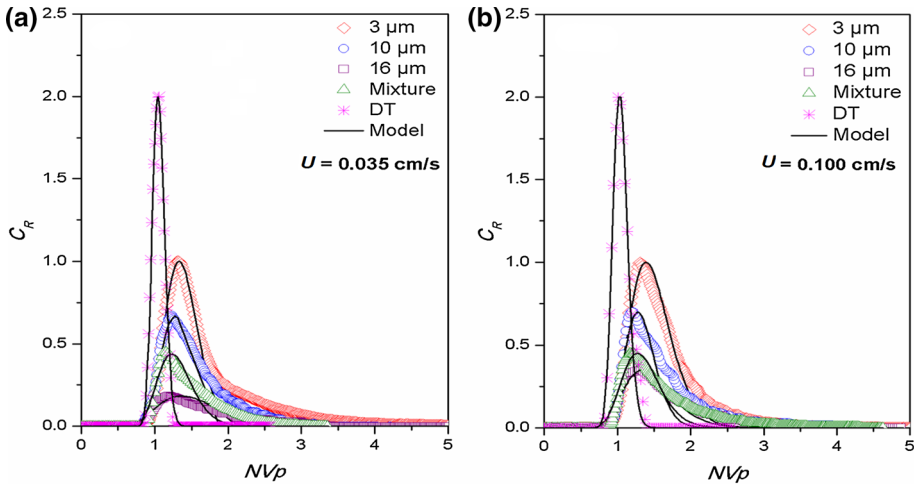
Fig. 1 Experimental and simulated breakthrough curves of the suspended particles and the dissolved tracer (DT) for flow velocities: **a** $U = 0.035$ cm/s and **b** $U = 0.100$ cm/s
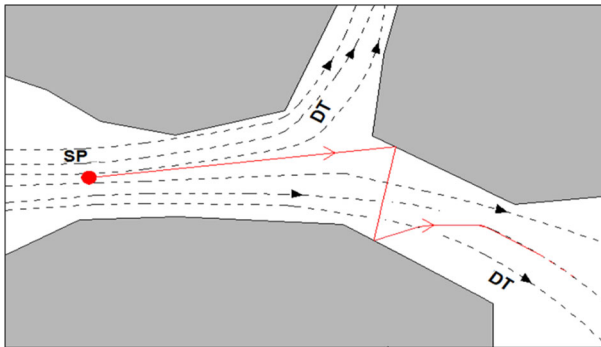

Fig. 2 Comparison of the suspended particles (SP) trajectory (after collision with the porous medium grains) with that of the dissolved tracer (DT)

by collisions between particles and the grains of the porous medium which can complicate and lengthen the transport paths of particles before reaching the column outlet.

The effect of particle sizes on the retardation is negligible when the flow velocities were less than 0.12 cm/s. Beyond this velocity (0.12 cm/s), the retardation factor is high only for the smallest SP studied (3 μm) compared to others SP populations (10 and 16 μm). For small particles, the transport paths that can be sampled by these ones are numerous. The transport paths become more tortuous, and the collision (SP grains) possibilities are more important leading to a significant lengthening of the transport paths. However, the large particles are excluded from small pores (size exclusion effects) and they are transported more rapidly within the porous medium when they are not trapped. Similar behaviour was observed by earlier works (Bradford et al. 2003; You et al. 2013).

Figure 4 shows the evolution of the longitudinal hydrodynamic dispersion coefficient D_L for both SP and DT as function of the average pore velocity u. For a given SP population, D_L increases with the average pore flow velocity u following a power law ($D_L = \alpha_L u^m$), with
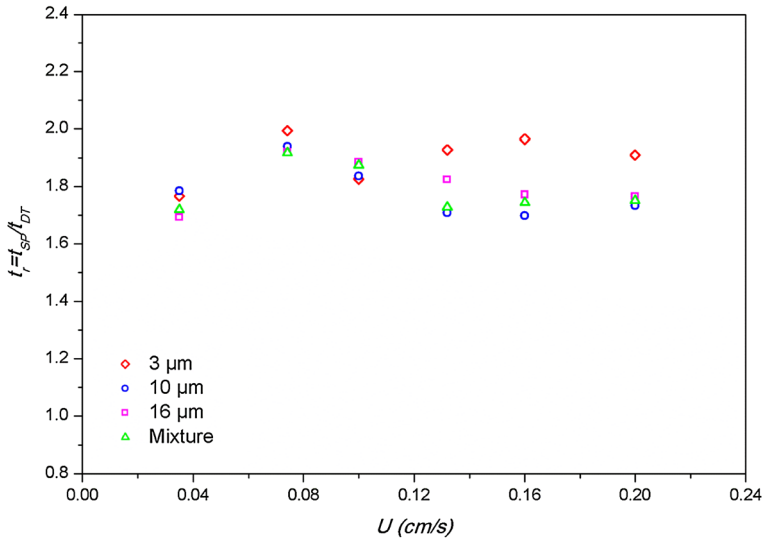
Fig. 3 Evolution of the retardation factor (t_r) versus Darcy's velocity (U) for the four used suspended particles populations
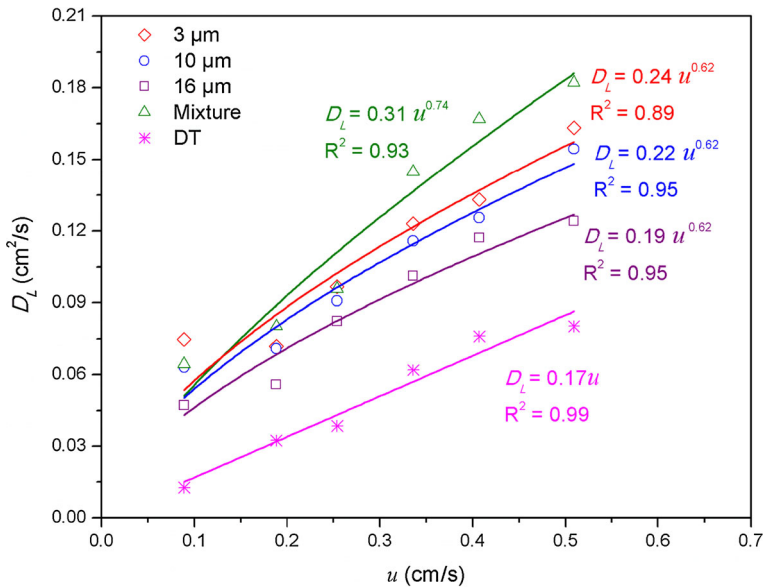

Fig. 4 Longitudinal dispersion coefficient D_L as function of the average pore velocity u for all tested particles populations (3, 10, 16 µm, and Mixture) and for dissolved tracer (DT)

a_L being the longitudinal dispersivity and m being an empirical power coefficient. However, a linear behaviour is obtained for the DT as it is often assumed in the literature (Pfannkuch 1963; Bear 1972). The values of m are ranged between 0.58 and 0.65 with an average value of 0.62 for the monodisperse SP populations and 0.74 for the SP mixture.
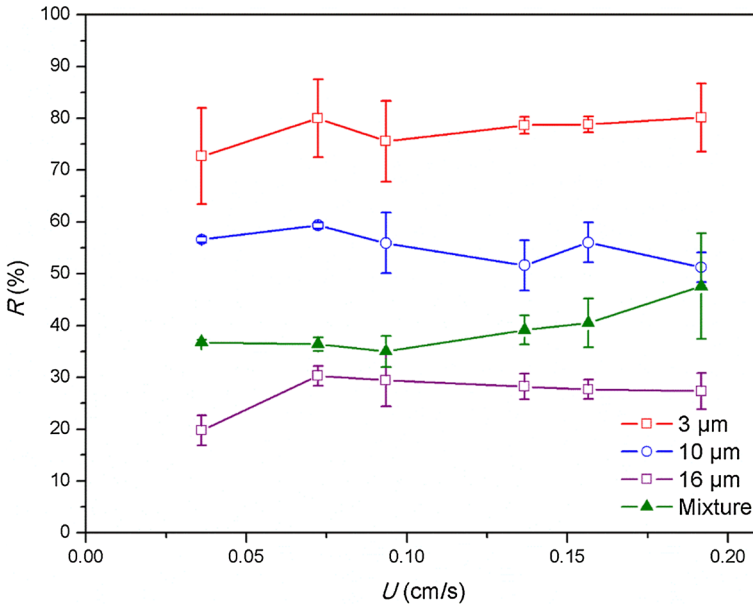
Fig. 5 SP recovery rate $R(\%)$ as a function of Darcy velocity U for the four used populations

The longitudinal dispersivity coefficient D_L of the DT is 1.5–3.5 times lower than that of the SP over all tracer experiments. This behaviour can be related to the multiple collisions experienced within the porous medium by the transported SP which increases their dispersion.

The longitudinal hydrodynamic dispersion coefficient D_L decreases as particle size increases for monodisperse populations. This result was observed by other authors (Auset and Keller 2004; Syngouna and Chrysikopoulos 2011). The large particles are excluded from small pores and from a certain number of tortuous paths and sample the pores with interstitial flow velocities more favourable for their transport to the outlet of porous medium. During transfer, the large particles remain in the pore centre and follow the less tortuous paths. So they are less dispersed than the smaller ones. In addition, as reported by Chrysikopoulos and Katzourakis (2015), the decreasing of D_L with particle size increasing may be due to the extensive particle retention. However, some earlier works (Bennacer et al. 2013; Chrysikopoulos and Katzourakis 2015) revealed a high dispersivity of large particles compared to smaller ones. Chrysikopoulos and Katzourakis (2015) attributed this behaviour to the combined effects of reduction in the colloid effective porosity that leads to tortuosity changes, possible existence of preferential flow paths, and exclusion from the lower velocity regions.

Figure 4 shows that the longitudinal dispersivity coefficient D_L of mixture is slightly higher than D_L of monodisperse populations, especially for higher flow velocities. Thus, a large particle size distribution leads to higher particle dispersion in the porous medium.

3.2 Influence of Particle Size Non-Uniformity

Figure 5 shows the evolution of the recovery rate $R(\%)$ as a function of Darcy's velocity U for all tested SP populations. The recovery rate of the SP, presented in this paper, is estimated by integrating the experimental BTCs ($\int_0^\infty C_R.dNVp = R$). Results show that the recovery

rate is almost unchangeable (does not change significantly) with the flow velocity. Results reveal the importance of the injected particles size in their transport and deposition in porous medium. Because of their density close to that of water, the gravity effect is negligible. Straining is the dominant mechanism for SP retention. In the present study, the ratio d_p/d_g of the SP 3, 10, and 16 μm is greater than 0.004, 0.014, and 0.022, respectively. These values are significantly higher than the 0.003 reported by Bradford et al. (2007). Indeed, Bradford (2007) reported that straining can play a very significant role in colloid deposition when d_p/d_g is as low as 0.003. No noticeable influence of the flow velocity on the SP recovered was observed, meaning that the flow velocity effect on the SP retention is limited. Whatever the flow velocity, the recovery rate of the particles constituting the Mixture population is lower than that obtained from the experiments performed with monodisperse particle populations 3 and 10 μm. However, Mixture population recovery rate is higher than that obtained from the experiments performed with 16 μm particles. These results show that the largest population (16 μm) dominate the behaviour of the mixture, despite the large number of the particles of 3 and 10 μm compared to this of the particles 16 μm.

As mentioned in sect. 2.1, Mixture population injections were performed to evaluate the effect of SP polydispersivity on their transport and deposition. Measurement of the number of the SP injected and recovered for the experiments with monodisperse and polydisperse (Mixture) particles were carried out with the help of the Coulter Multisizer counter. Following those measurements, Fig. 6 depicts the recovery rate ($R(\%)$) of the 3, 10, and 16 μm populations in monodisperse experiments (red bars) and those with the Mixture population in mixture experiments (blue bars). Whatever the flow velocity, the recovery rate of the particles 3 μm in the mixture experiments is always lower than that obtained in the monodisperse experiments. For example, when the flow velocity $U = 0.035$ cm/s, the recovery rate of the particle of 3 μm in monodisperse experiment is around $R = 73\%$, and it decreases to around $R = 44\%$ in the mixture experiments. However, the recovery rates of 10 and 16 μm populations are slightly enhanced in the mixture experiments compared to those realized in monodisperse experiments.

One possible explanation of this behaviour is that retention of large particles (10 and 16 μm) by straining in the pores which could be accessible to 3 μm particles reduces the size of pores openings. As a consequence, retention of small particles (3 μm) is enhanced by straining. On the other hand, for the populations 10 and 16 μm, a possible interpretation is that the deposition of 3 μm particles, which are the most numerous in Mixture population, depleted the porous medium capacity to retain the other large size particles. The strong improvement in the deposition of 3 μm particles saturated the available retention sites in the porous medium. These results are consistent with those obtained by Brow et al. (2005) and Xu and Saiers (2009) who showed that large particles tend to settle to the access pores reducing the pore size, thereby improving the retention of small particles. This analysis also explains the result shown in Fig. 6 dealing with the overall recovery rates of the Mixture population.

The evolution of the deposition kinetics coefficient K_{dep} as a function of the ratio of d_p/d_g is depicted in Fig. 7a for all flow velocities tested. For the Mixture population, an equivalent diameter corresponding to the weighted average diameter by mass of the populations 3, 10, and 16 μm is considered ($d_p = 9.7$ μm). K_{dep} increases with increasing flow velocity. For a given flow velocity, K_{dep} increases with the particle size. This result was expected to the extent that retention of the SP in this study is dominated by straining. Thus, the deposition kinetics coefficient K_{dep} is due mainly to straining. A linear evolution of K_{dep} with the particle size can be considered ($K_{dep} = \alpha(d_p/d_g)$). Bradford et al. (2003) proposed a power relationship between the deposition kinetics coefficient by straining and the ratio d_p/d_g
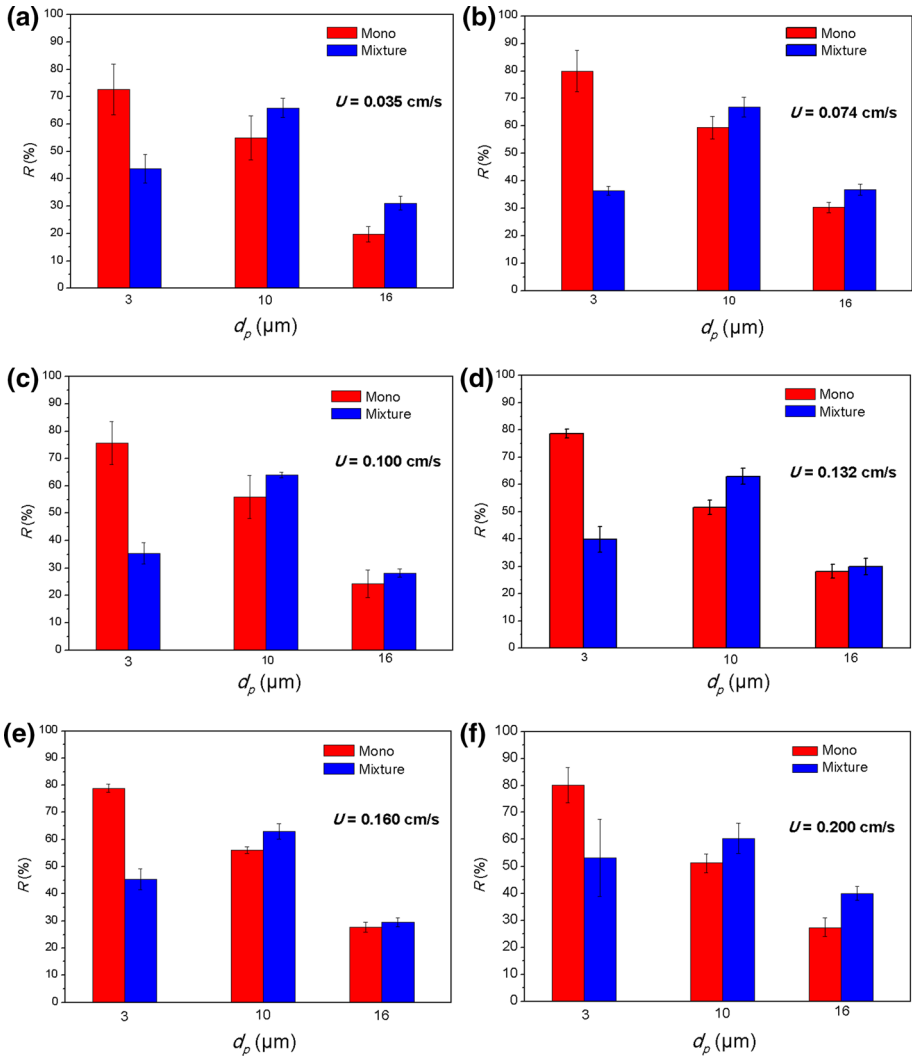
Fig. 6 Comparison of the suspended particles recovery rate of monodisperse particles injected in "monodisperse experiments" (*red bars*) with the recovery rates of different populations constituting the Mixture population in "mixture experiments" (*blue bars*) at different flow velocities: **a** $U = 0.035$ cm/s, **b** $U = 0.074$ cm/s, **c** $U = 0.100$ cm/s, **d** $U = 0.132$ cm/s, **e** $U = 0.160$ cm/s, and **f** $U = 0.200$ cm/s

$[K_{dep} = \alpha(d_p/d_g)^n]$. Other authors (Xu et al. 2006; Porubcan and Xu 2011; Raychoudhury et al. 2014) suggest a linear relationship between the K_{dep} and d_p/d_g. In our study, the results show that the coefficient α increases linearly with flow velocity ($\alpha = 3.52U$ [T^{-1}]). Figure 7b summarizes the simultaneous effects of the flow velocity and the ratio of d_p/d_g on the deposition kinetics coefficient. Thus, the influences of both particle size diameter and flow velocity on SP deposition "by straining" can be described by the following relationship:

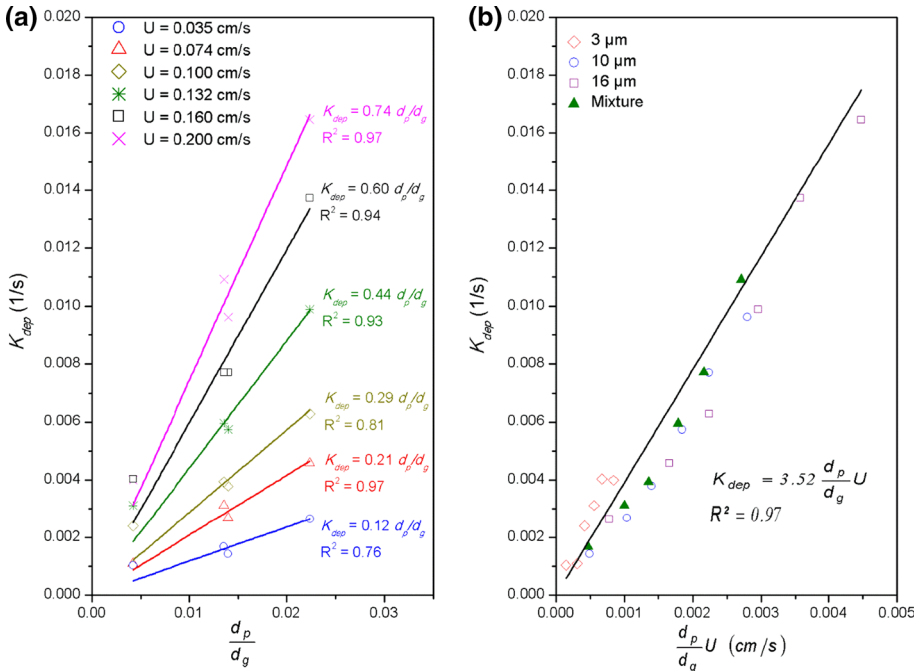$$K_{dep} = 3.52\frac{d_p}{d_g}U \qquad (4)$$

Fig. 7 **a** Evolution of the deposition kinetics coefficient K_{dep} as a function of the ratio of d_p/d_g at different flow velocities. **b** Simultaneous effects of the flow velocity and the particles sizes (presented by the ratio of d_p/d_g) on the deposition kinetics coefficient

This evolution of K_{dep} is similar to that proposed by Foppen et al. (2005) who studied Escherichia coli straining in two different sands under several flow velocities.

4 Conclusion

In this paper, particle size non-uniformity effects on the suspended particles transport and deposition in saturated porous media are investigated under different flow velocities. Previous researches demonstrate that solid particles transport and deposition are sensitive to certain parameters, such as the pore flow velocity, water ionic strength, and particle sizes (straining). In our study, the obtained results suggest considering not only the particle sizes but also their polydispersivity (particles size distribution). Besides the fact that the polydisperse particles generate larger hydrodynamic dispersion in the porous medium compared to the transport of dissolved tracer, high flow velocities increase their dispersion relative to the transport of monodisperse particles. As expected, particles retention in the porous medium by straining depends on the particle sizes. However, the obtained results indicate that the particle retention by straining is sensitive to the interactions between the different sized particles (constituting the polydisperse particles) that enhance the retention of small particles within the porous medium. Therefore, the large particles strained in the pores that could be accessible to small ones promote the capture of these small particles by straining. A linear relationship describing the effect of both particle sizes and flow velocity on K_{dep} is proposed.

References

Ahfir, N.-D., Hammadi, A., Alem, A., Wang, H.-Q., Le Bras, G., Ouahbi, T.: Porous media grain size distribution and hydrodynamic forces effects on transport and deposition of suspended particles. J. Environ. Sci. (2016). doi:10.1016/j.jes.2016.01.032

Ahfir, N.D., Benamar, A., Alem, A., Wang, H.-Q.: Influence of internal structure and medium length on transport and deposition of suspended particles: a laboratory study. Transp. Porous Media **76**(2), 289–307 (2009)

Aim, R.B., Vigneswaran, S., Prasanthi, H., Jegatheesan, V.: Influence of particle size and size distribution in granular bed filtration and dynamic microfiltration. Water Sci. Technol. **36**, 207–215 (1997)

Alem, A., Elkawafi, A., Ahfir, N.-D., Wang, H.: Filtration of kaolinite particles in a saturated porous medium: hydrodynamic effects. Hydrogeol. J. **21**(3), 573–586 (2013)

Auset, M., Keller, A.: Pore-scale processes that control dispersion of colloids in saturated porous media. Water Resour. Res. **40**(12), W03503 (2004)

Bear, J.: Dynamics of Fluids in Porous Media. Elsevier, New York (1972)

Benamar, A., Wang, H.-Q., Ahfir, N.-D., Alem, A., Masséi, N., Dupont, J.-P.: Flow velocity effects on the transport and the deposition rate of suspended particles in a saturated porous medium. C. R. Geosci. **337**, 497–504 (2005)

Bennacer, L., Ahfir, N.D., Bouanani, A., Alem, A., Wang, H.-Q.: Suspended particles transport and deposition in saturated granular porous medium: particle size effects. Transp. Porous Media **100**(3), 377–392 (2013)

Bonelli, S., Brivois, O., Borghi, R., Benahmed, N.: On the modelling of piping erosion. C. R. Mecanique **334**, 555–559 (2006)

Bradford, S.A., Simunek, J., Bettahar, M., Van Genuchten, M.T., Yates, S.R.: Modeling colloid attachment, straining, and exclusion in saturated porous media. Environ. Sci. Technol. **37**(10), 2242–2250 (2003)

Bradford, S.A., Torkzaban, S., Walker, S.L.: Coupling of physical and chemical mechanisms of colloid straining in saturated porous media. Water Res. **41**, 3012–3024 (2007)

Bradford, S.A., Yates, S.R., Bettahar, M., Simunek, J.: Physical factors affecting the transport and fate of colloids in saturated porous media. Water Resour. Res. **38**(12), 1–12 (2002)

Brow, C.N., Li, X., Rička, J., Johnson, W.P.: Comparison of microsphere deposition in porous media versus simple shear systems. Coll. Surf. A Physicochem. Eng. Asp. **253**(1–3), 125–136 (2005)

Chen, H., Gao, B., Li, H., Ma, L.Q.: Effects of pH and ionic strength on sulfamethoxazole and ciprofloxacin transport in saturated porous media. J. Contam. Hydrol. **126**(1–2), 29–36 (2011)

Chen, X.X., Bai, B.: Experimental investigation and modeling of particulate transportation and deposition in vertical and horizontal flows. Hydrogeol. J. **23**(2), 365–375 (2015). doi:10.1007/s10040-014-1205-2

Chrysikopoulos, C.V., Katzourakis, V.E.: Colloid particle size-dependent dispersivity. Water Resour. Res. **51**(6), 4668–4683 (2015)

Clark, L.A., Wynn, T.M.: Methods for determining streambank critical shear stress and soil erodibility: implications for erosion rate predictions. Trans. ASABE **50**(1), 95–106 (2007)

Derjaguin, B., Landau, L.: Theory of the stability of strongly charged lyophobicsols and of the adhesion of strongly charged particles in solution of electrolytes. Acta Physicochim. **14**, 633–662 (1941)

Elimelech, M., Gregory, J., Jia, X., Williams, R.A.: Particle Deposition and Aggregation: Measurement, Modeling, and Simulation. Butterworth-Heinemann, Oxford (1995)

Foppen, J.W.A., Mporokoso, A., Schijven, J.F.: Determining straining of *Escherichia coli* from breakthrough curves. J. Contam. Hydrol. **76**(3–4), 191–210 (2005)

Grolimund, D., Elimelech, M., Borkovec, M., Barmettler, K., Kretzschmar, R., Sticher, H.: Transport of in situ mobilized colloidal particles in packed soil columns. Environ. Sci. Technol. **32**(22), 3562–3569 (1998)

Herzig, J.P., Leclerc, D.M., Le Goff, P.: Flow of suspension through porous media: application to deep bed filtration. Ind. Eng. Chem. **62**, 8–35 (1970)

James, S.C., Chrysikopoulos, C.V.: Analytical solutions for monodisperse and polydisperse colloid transport in uniform fractures. Coll. Surf. A Physicochem. Eng. Asp. **226**, 101–118 (2003)

James, S.C., Bilezikjian, T.K., Chrysikopoulos, C.V.: Contaminant transport in a fracture with spatially variable aperture in the presence of monodisperse and polydisperse colloids. Stoch. Environ. Res. Risk Assess. **19**(4), 266–279 (2005)

James, S.C., Chrysikopoulos, C.V.: Monodisperse and polydisperse colloid transport in water-saturated fractures with various orientations: gravity effects. Adv. Water Resour. **34**, 1249–1255 (2011)

Johnson, W.P., Li, X., Assemi, S.: Deposition and re-entrainment dynamics of microbes and non-biological colloids during non-perturbed transport in porous media in the presence of an energy barrier to deposition. Adv. Water Resour. **30**(6–7), 1432–1454 (2007)

Kretzschmar, R., Barmettler, K., Grolimund, D., Yan, Y.-D., Borkovec, M., Sticher, H.: Experimental determination of colloid deposition rates and collision efficiencies in natural porous media. Water Resour. Res. **33**(5), 1129 (1997)

Kretzschmar, R., Borkovec, M., Grolimund, D., Elimelech, M.: Mobile subsurface colloids and their role in contaminant transport. Adv. Agron. **66**, 121–193 (1999)

Lee, J., Koplik, J.: Network model for deep bed filtration. Phys Fluids **13**, 1076–1086 (2001)

Masséi, N., Lacroix, M., Wang, H.Q., Dupont, J.P.: Transport of particulate material and dissolved tracer in a highly permeable porous medium: comparison of the transfer parameters. J. Contam. Hydrol. **57**(1–2), 21–39 (2002)

McCarthy, J.F., McKay, L.D.: Colloid transport in the subsurface: past, present, and future challenges. Vadose Zone J. **3**, 326–337 (2004)

McDowell-Boyer, L.M., Hunt, J.R., Sitar, N.: Particle transport through porous media. Water Resour. Res. **22**, 1901–1921 (1986)

Mesticou, Z., Kacem, M., Dubujet, P.: Coupling effects of flow velocity and ionic strength on the clogging of a saturated porous medium. Transp. Porous Media **112**(1), 265–282 (2016)

Moghadasi, J., Müller-Steinhagen, H., Jamialahmadi, M., Sharif, A.: Model study on the kinetics of oil field formation damage due to salt precipitation from injection. J. Pet. Sci. Eng. **43**(3–4), 201–217 (2004)

Pfannkuch, H.O.: Contribution à l'étude des déplacements de fluides miscibles dans un milieu poreux. Revue Française de l'institut du Pétrole **18**, 215–270 (1963)

Porubcan, A., Xu, S.: Colloid straining within saturated heterogeneous porous media. Water Res. **45**(4), 1796–1806 (2011)

Raychoudhury, T., Tufenkji, N., Ghoshal, S.: Straining of polyelectrolyte-stabilized nanoscale zero valent iron particles during transport through granular porous media. Water Res. **50**, 80–89 (2014)

Ryan, J.N., Elimelech, M.: Colloid mobilization and transport in groundwater. Coll. Surf. A Physicochem. Eng. Asp. **107**(95), 1–56 (1996)

Sadiq, R., Husain, T., Al-Zahrani, A.M., Sheikh, A.K., Farooq, S.: Secondary effluent treatment by slow sand filters: performance and risk analysis. Water Air Soil Pollut. **143**, 41–63 (2003)

Sefrioui, N., Ahmadi, A., Omari, A., Bertin, H.: Numerical simulation of retention and release of colloids in porousmedia at the pore scale. Coll. Surf. A: Physicochem. Eng. Asp. **427**, 33–40 (2013)

Sen, T.K., Khilar, K.C.: Review on subsurface colloids and colloid-associated contaminant transport in saturated porous media. Adv. Coll. Interface Sci. **119**(2–3), 71–96 (2006)

Sen, T.K., Mahajan, S.P., Khilar, K.C.: Colloid-Associated contaminant transport in porous media: 1 Experimental studies. AIChE J. **48**(10), 2366–2374 (2002)

Sjödahl, P., Dahlin, T., Johansson, S., Loke, M.H.: Resistivity monitoring for leakage and internal erosion detection at Hällby embankment dam. J. Appl. Geophys. **65**(3–4), 155–164 (2008)

Syngouna, V.I., Chrysikopoulos, C.V.: Transport of biocolloids in water saturated columns packed with sand: Effect of grain size and pore water velocity. J. Contam. Hydrol. **126**, 301–314 (2011)

Syngouna, V.I., Chrysikopoulos, C.V.: Cotransport of clay colloids and viruses in water saturated porous media. Coll. Surf. A Physicochem. Eng. Asp. **416**, 56–65 (2013)

Tong, M., Johnson, W.P.: Excess colloid retention in porous media as a function of colloid size, fluid velocity, and grain angularity. Environ. Sci. Technol **40**, 7725–7731 (2006)

Torkzaban, S., Kim, H.N., Simunek, J., Bradford, S.A.: Hysteresis of colloid retention and release in saturated porous media during transients in solution chemistry. Environ. Sci. Technol. **44**(5), 1662–1669 (2010)

Tosco, T., Sethi, R.: Transport of non-Newtonian suspensions of highly concentrated micro- and nanoscale iron particles in porous media: A modeling approach. Environ. Sci. Technol. **44**(23), 9062–9068 (2010)

Verwey, E.J.W., Overbeek, J.T.H.G.: Theory of the Stability of Lyophobic Colloids. Elsevier, Amsterdam (1948)

Walshe, G.E., Pang, L., Flury, M., Close, M.E., Flintoft, M.: Effects of pH, ionic strength, dissolved organic matter, and flow rate on the co-transport of MS2 bacteriophages with kaolinite in gravel aquifer media. Water Res. **44**(4), 1255–1269 (2010)

Wang, H.Q., Lacroix, M., Masséi, N., Dupont, J.-P.: Particle transport in a porous medium: determination of hydrodispersive characteristics and deposition rates. C. R. Acad. Sci. Paris Earth Planet. Sci. **331**, 97–104 (2000)

Xu, S.P., Liao, Q., Saiers, J.E.: Straining of nonspherical colloids in saturated porous media. Environ. Sci. Technol. **42**, 771–778 (2008)

Xu, S.P., Saiers, J.E.: Colloid straining within water-saturated porous media: effects of colloid size nonuniformity. Water Resour. Res. **45**, W05501 (2009)

Xu, S., Gao, B., Saiers, J.E.: Straining of colloidal particles in saturated porous media. Water Resour. Res. **42**(12), 1–10 (2006)

You, Z., Badalyan, A., Bedrikovetsky, P.: Size-exclusion colloidal transport in porous media: stochastic modeling and experimental study. Soc. Pet. Eng. **18**(4), 620–633 (2013)